Numerical study of the late stages of spinodal decomposition

T. M. Rogers, K. R. Elder, and Rashmi C. Desai
Department of Physics, University of Toronto, Toronto, Ontario, Canada M5S 1A7
(Received 14 September 1987)

A numerical simulation of a two-dimensional system with a continuous order parameter (model *B*) is used to study phase separation for a critical quench. Domain growth and scaling are investigated through the pair correlation function. At late stages, the characteristic domain size grows as $R(t) \sim t^{1/3}$. It is only in this time regime that scaling of the correlation function is established. The scaling function and the asymptotic growth law are found to be independent of the strength of thermal fluctuations. Details of the finite-difference scheme used to simulate the dynamics are discussed.

I. INTRODUCTION

Pattern formation in phase separation is a problem of longstanding perplexity. When a system, initially in a homogeneous equilibrium state, is rapidly cooled (quenched) into the two-phase coexistence region, small spatial inhomogeneities in the order parameter evolve into macroscopic domains, and eventually, into a two-phase equilibrium state. A rough distinction can be drawn between nucleation and spinodal decomposition, depending on whether the quench leaves the system in a metastable or unstable state. The phenomenon, ubiquitous in physics, chemistry, and metallurgy, has been studied extensively.[1] Recently, much controversy has erupted with respect to the late stages,[2–24] which can be characterized by the coarsening of domains separated by interfaces. There is evidence of universality in this time regime, in the sense that some properties do not depend on the detailed microscopics. Although the delineation of universality classes is not fully understood, the symmetry of the order parameter and the existence of conservation laws seem to play a major role.

In this paper, the case of a scalar conserved order parameter is considered. For such a system, both experiments[20–24] and computer simulations[11–19] suggest that the topology scales with time. In particular, during late stages of coarsening, the spatial patterns at two different times are related by a global change of the length scale. The emergence of scaling is a result of a single length dominating the dynamics. An important quantity relating experiments, simulations, and theories is the time-dependent structure factor, $S(k,t)$, which measures the strength of spatial correlations in the order parameter with wave vector k, at time t. A signature of scaling is the fact that the structure factor can be cast in the form

$$S(k,t)=R^d(t)S_0(kR(t)) , \tag{1.1}$$

where S_0 is a time-independent function and $R(t)$ is a characteristic length of the system (such as the average domain size). The time dependence of R, and the extent of universality, have become intensely debated questions.

For a nucleating system, the classic work of Lifshitz and Slyosov[2] on cluster growth forms the theoretical focus. They developed a description of coarsening based on an evaporation-condensation mechanism, whereby larger clusters grow at the expense of smaller ones. The growth is mediated by the surface tension. Their asymptotic analysis predicts a power-law growth in time for the average cluster radius: $R \sim t^n$, where n is $\frac{1}{3}$. This theory, and later extensions to it,[5,6] rely on a small volume fraction of one phase with respect to the other. Cluster coalescences are important for concentrated mixtures of the two phases,[7,9] and can affect the exponent, n.

During a critical quench (i.e., spinodal decomposition), a percolating cluster is formed and it is not obvious that the Lifshitz-Slyosov theory should apply. Along a different vein, approximate theories for the evolution of the structure factor[8–10,19] yield an exponent of $\frac{1}{4}$ (which should probably be interpreted as an intermediate-time result). In addition, Huse[11] has given a dimensional argument for expecting $n=\frac{1}{3}$ at late times, while a renormalization-group calculation by Mazenko *et al.*[12] gives logarithmic growth near zero temperature, for activated diffusion. Comparatively little is known about the role of fluctuations.

Considerable computer effort has also been brought to bear on the problem. Lebowitz *et al.*[13] used a spin-exchange kinetic Ising model to study phase separation. They first demonstrated that the structure factor scales with time and measured a growth exponent ranging from 0.19 to 0.35 depending on the depth of the quench and the degree of off-criticality. Further Ising simulations[11,12] led to conflicting interpretations. Recently, a detailed study[14] has shown a time-dependent exponent asymptotically approaching $\frac{1}{3}$, confirming the work of Huse.[11] In molecular-dynamics simulations,[15] $n=\frac{1}{3}$ has been seen, although with the introduction of Langevin noise[16] the exponent becomes $\frac{1}{4}$ over the same time scales.

A difficulty with these microscopically based simulations is the extensive computer time required to probe late-stage coarsening. There has been mounting interest in using numerical simulations based on a coarse-grained description of the order parameter, which has the advantage of making larger time scales accessible. (This approach has already proved successful for the case of a nonconserved order parameter.[17,25,26]) In Ref. 27, such investigations were initiated, although the authors did not look at domain growth and scaling. Preliminary in-

vestigations of late-stage phenomena have been reported for Monte Carlo[18] and Langevin dynamics.[19] In addition, a coupled map scheme with conserved dynamics[17] has been developed to study the problem.

In this paper, a numerical study of domain coarsening in spinodal decomposition is presented for a diffusive system with a conserved order parameter (model B). The approach is similar to investigations of Oppo and Kapral[25] for the nonconserved case. Particular attention is paid to the time dependence of the characteristic length scale and the onset of scaling. The simulations yield a late-stage growth exponent of $\frac{1}{3}$. A power-law ansatz for the growth at intermediate times leads to an "effective exponent" which changes continuously with time. Scaling is only established asymptotically. Thermal fluctuations seem to have no effect on the asymptotic growth law or the scaling function. However, the strength of the noise does change the approach to the late-stage growth and affects corrections to scaling. Some important technical considerations in the implementation of the numerical scheme are also discussed.

II. COMPUTER SIMULATION

The theoretical framework for understanding the dynamics of spinodal decomposition is based primarily on the formulations[28] of Cahn and Hilliard and of Cook. They developed a phenomenological equation for the time evolution of the order-parameter fluctuations, $\phi(\mathbf{r},t)$, which is referred to as model B in the scheme of critical dynamics. Namely,

$$\frac{\partial\phi(\mathbf{r},t)}{\partial t}=M\nabla^2\frac{\delta F}{\delta\phi}+\zeta(\mathbf{r},t)\ , \tag{2.1}$$

where M is the mobility. The theory introduces a coarse-grained free energy F, which is a functional of the local order parameter. For a critical quench, F must exhibit a symmetric double-well structure. It is usual to employ the Ginzburg-Landau-Wilson form

$$F=\tfrac{1}{2}\int d\mathbf{r}\left[-r\phi^2+\frac{u}{2}\phi^4+\kappa(\nabla\phi)^2\right]\ , \tag{2.2}$$

where r, u, and κ are positive (phenomenological) constants. (For an off-critical system, there would be an additional term proportional to ϕ^3, which is not considered here.) The thermal noise $\zeta(\mathbf{r},t)$ satisfies the fluctuation-dissipation relationship,

$$\langle\zeta(\mathbf{r},t)\zeta(\mathbf{r}',t')\rangle=-2k_BTM\nabla^2\delta(\mathbf{r}-\mathbf{r}')\delta(t-t')\ . \tag{2.3}$$

Here k_B is Boltzmann's constant and T is the temperature. Reference 1 gives an excellent introduction to the vast literature on the derivation of and approximate solutions to model B.

Following the notation of Grant *et al.*,[29] Eqs. (2.1)–(2.3) can be put in the dimensionless form

$$\frac{\partial\psi}{\partial\tau}=\tfrac{1}{2}\nabla^2(-\psi+\psi^3-\nabla^2\psi)+\sqrt{\epsilon}\mu\ , \tag{2.4}$$

with

$$\langle\mu(\mathbf{x},\tau)\mu(\mathbf{x}',\tau')\rangle=-\nabla^2\delta(\mathbf{x}-\mathbf{x}')\delta(\tau-\tau')\ , \tag{2.5}$$

where

$$\mathbf{x}=\left[\frac{r}{\kappa}\right]^{1/2}\mathbf{r}\ ,$$

$$\tau=\left[\frac{2Mr^2}{\kappa}\right]t\ ,$$

$$\psi=\left[\frac{u}{r}\right]^{1/2}\phi\ ,$$

and

$$\epsilon=\frac{k_BTu}{r^2}\left[\frac{r}{\kappa}\right]^{d/2}\ .$$

The transformation emphasizes the fact that model B contains only one dimensionless parameter, ϵ, which characterizes the strength of the noise. (For fixed ϵ, variations of r, u, and κ can be absorbed into a unified description by appropriate rescaling of space and time.) The zero-temperature limit of the model corresponds to $\epsilon=0$. The magnitude of ϵ increases with temperature. Near the critical point ($r\to0$), ϵ diverges for $d<4$. In the language of critical phenomena, $\epsilon=0$, corresponds to the mean-field limit.

The simulations reported here adopt a finite-difference approximation for both the spatial and temporal derivatives in Eqs. (2.4) and (2.5). In two dimensions, the resulting discretized equation is

$$\psi_{i,j}(n)=\psi_{i,j}(n-1)+\frac{\Delta\tau}{2\Delta x^2}\sum_{\mathrm{NN}}\left[-\psi_{i,j}(n-1)+\psi_{i,j}^3(n-1)-\frac{1}{\Delta x^2}\sum_{\mathrm{NN}}\psi_{i,j}(n-1)\right]+\eta_{i,j}(n-1)\ . \tag{2.6}$$

The order parameter ψ is defined only on the sites $i,j\in[1,N]$ of a square lattice. The summation over nearest neighbors (NN) is such that

$$\sum_{\mathrm{NN}}f(\psi_{i,j})=f(\psi_{i+1,j})+f(\psi_{i-1,j})+f(\psi_{i,j+1})+f(\psi_{i,j-1})-4f(\psi_{i,j})\ , \tag{2.7}$$

for an arbitrary function $f(\psi)$. The value of $\{\psi_{i,j}\}$ at a given iteration, n, depends upon $\{\psi_{i,j}\}$ at the previous iteration as well as the thermal noise $\{\eta_{i,j}\}$. Unlike Ising simulations, here ψ is a continuous variable, with equilibrium values of ±1 corresponding to the wells of the free-energy functional defined in Eq. (2.2).

The fluctuation-dissipation relation for the discrete equation can be maintained by producing two independent Gaussian random variables $\nu^{(1)},\nu^{(2)}$ at each lattice site,[27] such that

$$\eta_{i,j}=\frac{1}{\Delta x}(\nu^{(1)}_{i+1,j}-\nu^{(1)}_{i,j}+\nu^{(2)}_{i,j+1}-\nu^{(2)}_{i,j}) , \tag{2.8}$$

where

$$\langle \nu^{(a)}_{i,j}(n)\nu^{(b)}_{k,l}(m)\rangle=\frac{\epsilon\Delta\tau}{(\Delta x)^d}\delta_{i,k}\delta_{j,l}\delta_{m,n}\delta_{a,b} .$$

The mapping manifestly obeys the conservation law appropriate for a critical quench,

$$\sum_{i,j}\psi_{ij}=0 . \tag{2.9}$$

The discretization scheme introduces a (dimensionless) time step, $\Delta\tau$, and a (dimensionless) mesh size, Δx. Connection with the continuous equations can be established by noting,

$$\tau=n\Delta\tau$$

and

$$\mathbf{x}=i\Delta x\hat{\mathbf{x}}+j\Delta x\hat{\mathbf{y}} .$$

The dynamical evolution of the discrete and continuous models, however, are not necessarily identical. For example, the discrete equations can undergo a subharmonic bifurcation for a certain range of Δx and $\Delta\tau$; whereas, this is not possible in the continuous equations. As a result, the time step and mesh size must be chosen carefully in order to establish a correspondence between the two models. These restrictions are discussed in Sec. III C.

III. RESULTS

We have investigated the dynamics of phase separation in the discrete model for a critical quench. The system was initially prepared in a homogeneous (single phase) state by assigning, to each lattice site, a random number uniformly distributed in the interval $[-\epsilon_0,+\epsilon_0]$. The magnitude of ϵ_0 reflects the strength of thermal fluctuations in the initial state. All computations were carried out on a two-dimensional square lattice with periodic boundary conditions. Throughout the remainder of the paper, the term "trial" refers to a single integration of the model for a given initial condition. A "run" involves an average over several different trials, each trial being started from its own random seed (i.e., an average over the noise). Tables I(a) and I(b) summarize the parameters used for each run.

A. Growth and scaling

The time evolution of the order parameter for a characteristic trial is shown in Fig. 1. In these snapshots, the shaded regions correspond to positive values of the order-parameter field. The symbol size at each lattice site is proportional to the magnitude of the field. [It should be noted that there is (statistical) symmetry of the field with respect to the spatial distribution of negative and positive values of the order parameter. In Fig. 1, however, regions where the order parameter is negative have been left blank.] The early stages of phase separation (not shown in the figure) involve the amplification of local fluctuations into large scale inhomogeneities. A detailed study of this process will be presented elsewhere. The late stages [Figs. 1(a)–1(c)] are characterized by domains (where ψ is near one of the two equilibrium values), separated by relatively sharp interfaces. Here the configurations exhibit an interwoven, connected topology which is common in spinodal decomposition.[1] The size of the domain increases with time as shown in these figures.

In order to make a quantitative analysis of domain growth, it is useful to focus on the pair correlation function,

TABLE I. (a) Parameters used in the simulations: effect of noise strength ϵ on phase separation (see text for definitions). (b) Parameters used in the simulations: effect of mesh size Δx and time step $\Delta\tau$.

Run	ϵ	ϵ_0	Δx	$\Delta\tau$	Size	N_{trials}[a]	n_{eff}[b]
				(a)			
A	0	0.05	1.7	0.3	100×100	126 ($\tau<900$)	
						26 ($\tau>900$)	0.32±0.01
B	0.05	0.05	1.7	0.3	124×124	20	0.32±0.01
C	0.2	0.05	1.7	0.06	124×124	10	0.31±0.02
D	0.5	0.05	1.7	0.02	124×124	7	0.27±0.02
				(b)			
E	0.05	0.0	0.7	0.01	100×100	1	
F	0.05	0.0	1.4	0.1	124×124	5	
G	0.05	0.0	1.9	0.3	124×124	2	
H	0.05	0.0	2.1	0.3	124×124	2	
I	0.05	0.0	2.3	0.3	124×124	2	
J	0.05	0.0	2.8	0.3	124×124	3	
K	0.05	0.05	1.7	0.03	124×124	2	

[a] N_{trials} refers to the number of trials used to average over the noise.
[b] Calculated for $\tau>900$ in runs *A*, *B*, *D*, and for $\tau>3000$ in run *C*.

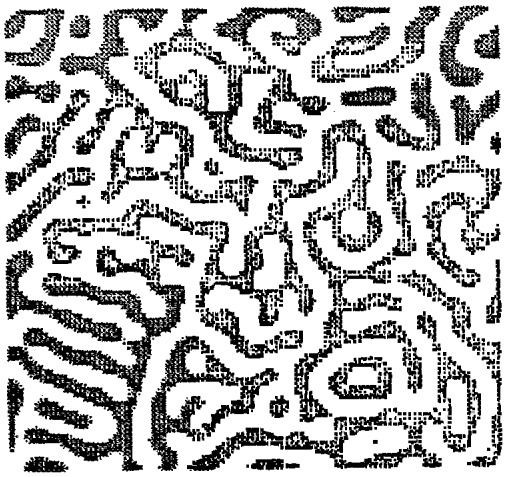

(a)

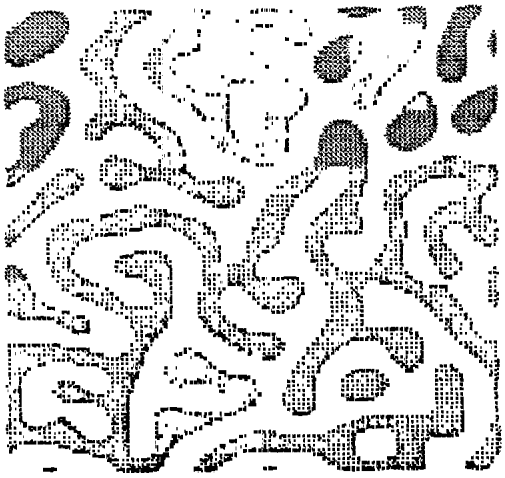

(b)

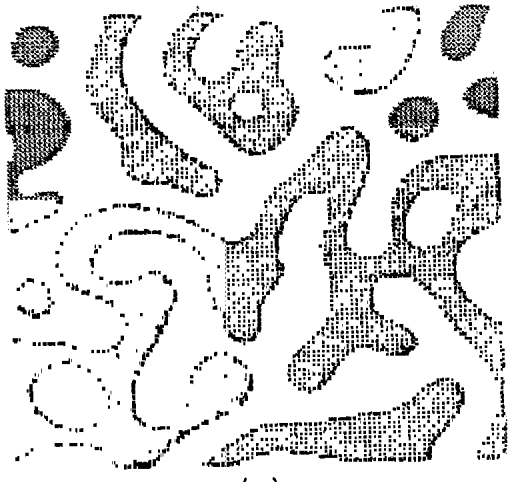

(c)

FIG. 1. Time evolution of the order-parameter field during phase separation in run A. The shaded regions correspond to $\psi>0$. (a), (b), and (c) correspond to $\tau=150$, 600, and 2200, respectively.

$$G(\mathbf{x},\tau)=\frac{1}{N^2}\sum_{\mathbf{x}'}\langle\psi(\mathbf{x}'+\mathbf{x},\tau)\psi(\mathbf{x}',\tau)\rangle\ , \tag{3.1}$$

where $\mathbf{x}$ is a lattice vector. The angular brackets in Eq. (3.1) denote an average over the thermal noise. If the system is isotropic then G depends only on the radial distance, $r=|\mathbf{x}|$. A further circular average leads to the radial pair correlation function,

$$g(r,\tau)=\frac{1}{N_r}\sum_{|\mathbf{x}|=r}G(\mathbf{x},\tau)\ , \tag{3.2}$$

where N_r is the number of lattice vectors of magnitude r. Figure 2 shows the typical dynamical evolution of the radial correlation function. The domain structure is apparent in the oscillations of the function about zero. As the system coarsens, spatial correlations extend increasingly further along the radial axis.

In the simulations, the distance at which $g(r,\tau)$ first crosses zero, $R_1(\tau)$, has been used as an arbitrary measure of domain size. To establish consistency, the second zero, $R_2(\tau)$, has also been determined. The zero was obtained by an interpolation of the datapoints over a region extending from the nearest minimum to the nearest maximum. Using the individual trials for run B, a standard deviation of 2% was obtained for R_1 and R_2. This result was used to estimate the statistical errors in all other runs.[30]

A logarithmic plot of the two radii as a function of time is given in Fig. 3 for run A. In this run there was no noise ($\epsilon=0$), consistent with the assumptions of Lifshitz

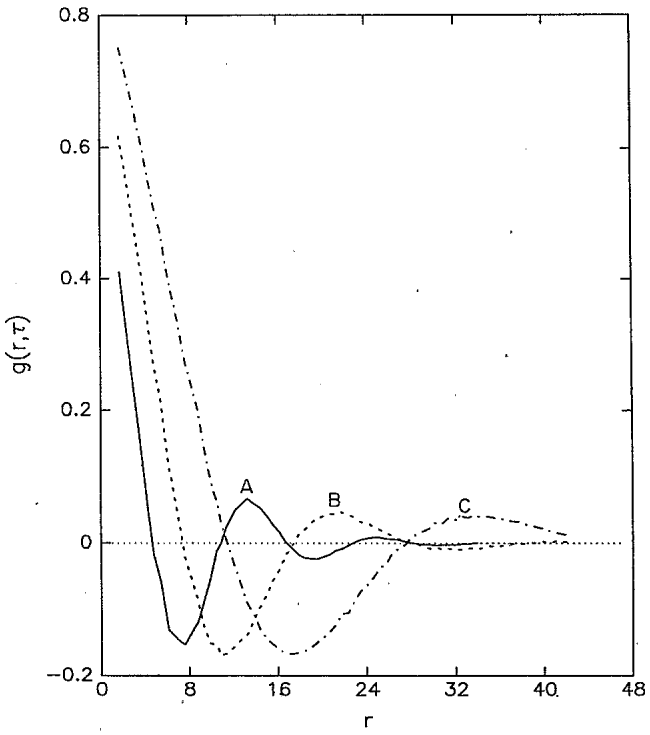

FIG. 2. Time dependence of the radial pair-correlation function in run A. The lines correspond to $\tau=150$ (A), $\tau=600$ (B), and $\tau=2400$ (C).

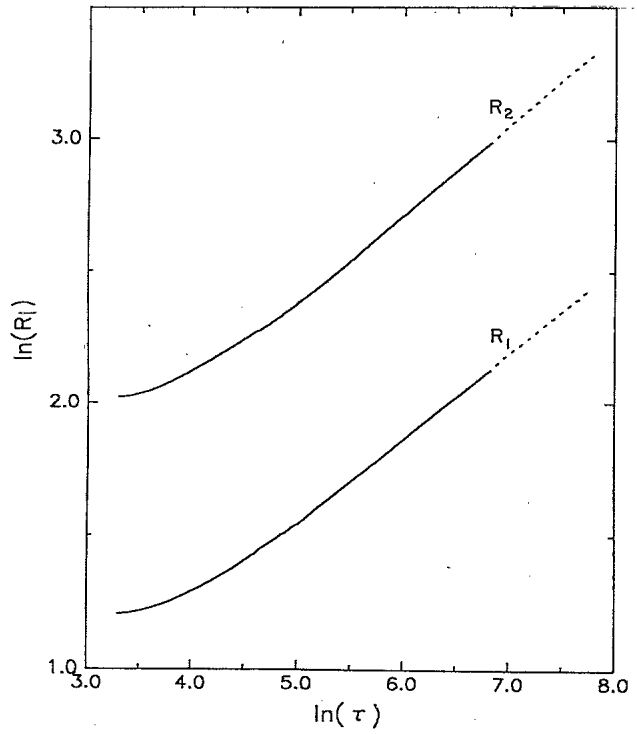

FIG. 3. The first zero and second zeros of $g(r,\tau)$ as a function of time in run A. (The data is plotted using natural logarithms.) The solid lines correspond to 126 trial averages; the dashed lines, 26.

and Slyosov.[2] (Randomness only enters through the initial conditions.) The datapoints for R_1 and R_2 are nearly (but not identically) parallel. It should be noted that if there is scaling, the ratio of the two lengths will be constant in time, leading to perfectly parallel lines. The instantaneous slope can be interpreted as an effective exponent, n_{eff}. The curvature in the plots for intermediate times indicates a continuous change of n_{eff}. At late stages, the data appear to be converging to a slope of $\frac{1}{3}$. A linear fit to the datapoints for $\tau > 900$ gives a slope of 0.32 ± 0.01 for both R_1 and R_2. Contrary to other studies, there is no convincing intermediate regime, where the slope levels off at $n_{\text{eff}} = \frac{1}{4}$. Rather, our data suggest a smooth and continuous approach to the asymptotic limit, $n = \frac{1}{3}$. It should be noted that because of the slow change of the (effective) exponent with time, it is easy to misinterpret intermediate time data to favor an asymptotic exponent which is lower than the true value. We believe that our simulations have probed a sufficiently large time scale to avoid this problem.

The intermediate stages of growth involve the establishment of broad domain walls, which then sharpen with time.[31] There is a correlation between the establishment of sharp walls and the onset of $n = \frac{1}{3}$. This was pointed out by Oono and Puri,[17] who associated an exponent of $\frac{1}{4}$ with "soft" (i.e., broad) walls and $\frac{1}{3}$ with "hard" (i.e., thin) walls. (The terminology is coined from Mouritsen's studies[32] of growth for a system with a nonconserved order parameter.) Although we do not see a well-defined region where $n = \frac{1}{4}$, it is clear from our simulations that the effective exponent is significantly smaller than $\frac{1}{3}$ when the domain walls are broad compared to the size of the domains.

The scaling ansatz for the pair-correlation function is

$$g(r,\tau) = f(z) , \tag{3.3}$$

where $z = r/R(\tau)$ and $R(\tau)$ is some characteristic length scale. The scaling function, $f(z)$, is time independent. The data for $R_1(\tau)$ have been used to test for scaling in the simulations. The results, for intermediate times, are shown in Fig. 4. There is no scaling here as evidenced by the change in shape of $f(z)$ with time. The minima and maxima of the function are slowly changing, and there is a shift of the second and third zeros with respect to the first. Figure 5 shows that further changes in the scaling function cannot be distinguished for $\tau > 900$. To within the accuracy of the statistics, the onset of scaling is coincident with the establishment of $n_{\text{eff}} = \frac{1}{3}$. The data suggest, in fact, that both are asymptotic results.

B. Effect of noise

The role of the thermal noise in domain growth and scaling was investigated in runs A, B, C, and D ($\epsilon = 0$, 0.05, 0.2, and 0.5, respectively). For nonzero ϵ, the spatial distribution of the domains in late-stage coarsening is qualitatively similar to the case for $\epsilon = 0$. A large percolating cluster forms, with an interwoven topology. The interfacial structure, however, is dependent on ϵ as illustrated in Fig. 6. This snapshot corresponds to $\epsilon = 0.5$. By comparison with Fig. 1, it is evident that increasing the strength of the noise leads to a rougher domain topology, with broader and more diffuse interfaces.

Logarithmic plots of R_1 as a function of τ for the four runs are shown in Fig. 7. The domain growth is faster for larger ϵ, indicating that fluctuations facilitate phase separation (especially for early and intermediate times). The plots appear to converge to the same slope at late times. The last column in Table I(a) gives the effective exponent of each run for the latest time scales probed. Within the accuracy of our statistics, the exponent has reached $\frac{1}{3}$ for $\epsilon = 0$, 0.05, and 0.2. (The effective exponent is slightly less than $\frac{1}{3}$ for $\epsilon = 0.5$, which suggests that the asymptotic growth regime has not been reached.) We conclude that the noise has no effect on the late-stage growth exponent. However, the approach to this asymptote is ϵ dependent. In particular, the transition is slower for larger noise strengths. [This is possibly an interpretation of the molecular dynamics simulations of Refs. 15 and 16, which give an exponent of $\frac{1}{3}$ without noise and an (effective) exponent of $\frac{1}{4}$ with noise.]

Scaling of the pair-correlation function for nonzero ϵ follows a similar trend to Figs. 4 and 5 ($\epsilon = 0$). For intermediate times, the scaling ansatz breaks down. It is only in the late-stage regime, where the effective exponent approaches $\frac{1}{3}$, that scaling is obeyed by the system. A comparison of the late-stage scaling functions is given in Fig. 8. There is excellent agreement for $\epsilon = 0$, 0.05, and 0.2, indicating that the form of the (asymptotic) scaling function is independent of the strength of the noise. The dot-

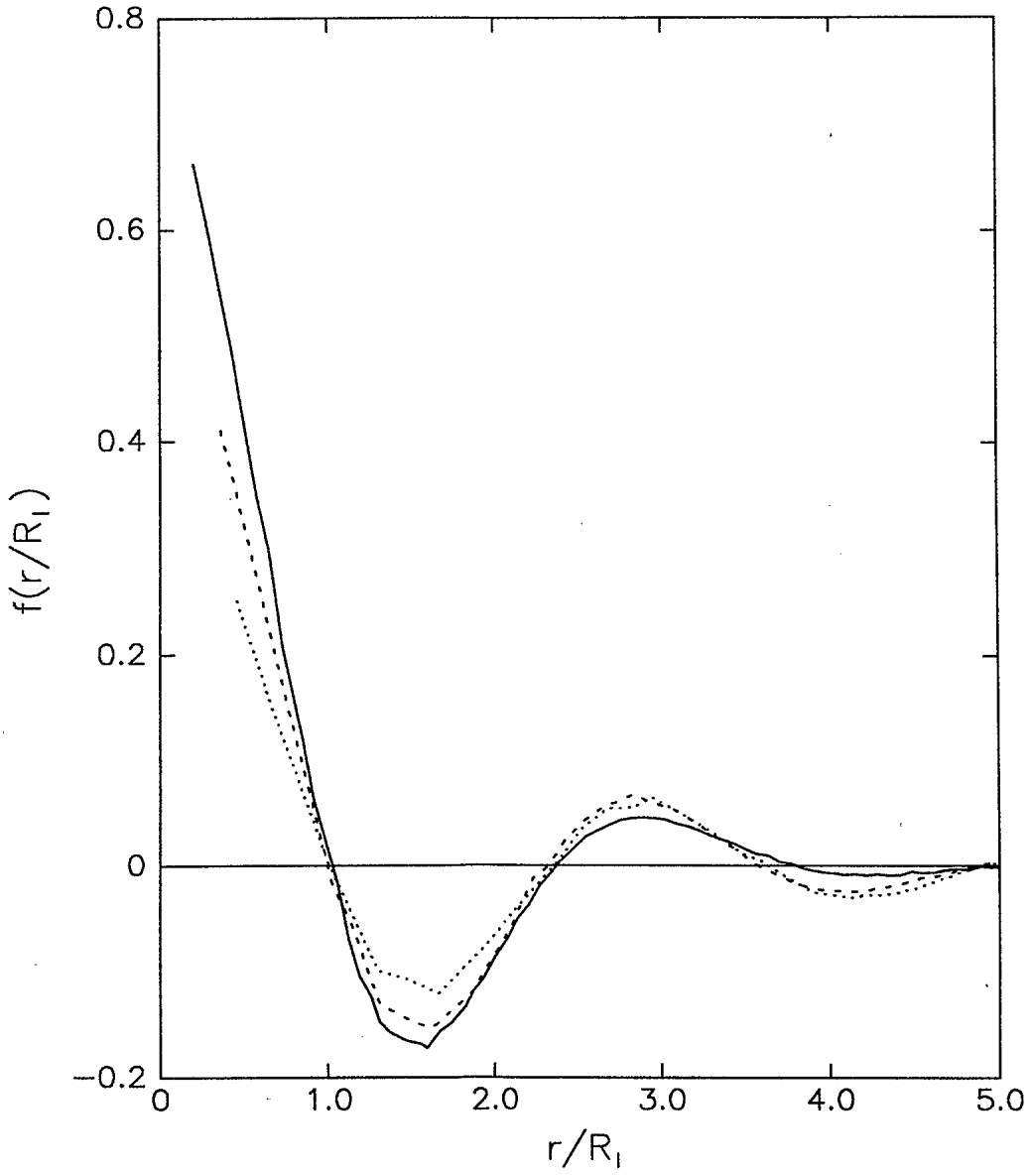

FIG. 4. The scaled correlation function for intermediate stages in run A. The data is plotted for $\tau=60$ (dotted line), $\tau=150$ (dashed line), and $\tau=900$ (solid line). There is no scaling in this time regime.

ted line on the graph corresponds to the latest time examined for $\epsilon=0.5$. There is a clear mismatch of this data, since the simulation has not reached the late-stage scaling regime. This interpretation is consistent with the fact that, for this run, the effective exponent is less than $\frac{1}{3}$ (Fig. 7).

C. Effect of $\Delta\tau$ and Δx

Equation (2.4) is a nonlinear stochastic diffusion equation which presents a challenging numerical problem. The choice of a finite-difference algorithm is based upon the constraints of a stochastic noise term[33] and the need for computer efficiency. The discretization scheme introduces two parameters, namely, the dimensionless time step $\Delta\tau$, and the dimensionless mesh size Δx. Some care must be taken with these parameters to avoid spurious solutions.

In the absence of noise, Eq. (2.6) becomes a spatially coupled map, similar to the nonconserved map studied in Ref. 25. It is insightful to adapt their linear stability analysis to study the bifurcation structure.

For a lattice of size $N\times N$, the Fourier transform of the order parameter is defined

$$\xi_{\mathbf{k}}=\frac{1}{N^2}\sum_{\mathbf{x}}\psi_{\mathbf{x}}e^{i\mathbf{x}\cdot\mathbf{k}}\ , \tag{3.4}$$

where the sum is over the lattice vectors. The Fourier modes are restricted to the reciprocal lattice,

$$\mathbf{k}=\frac{2\pi}{N\Delta x}(l\hat{\mathbf{x}}+m\hat{\mathbf{y}})\ , \tag{3.5}$$

where $l,m\in[1,N]$. The mesh size Δx has been explicitly incorporated here so that the continuous limit is transparent (i.e., $\Delta x\rightarrow 0$). In Fourier space, the map becomes

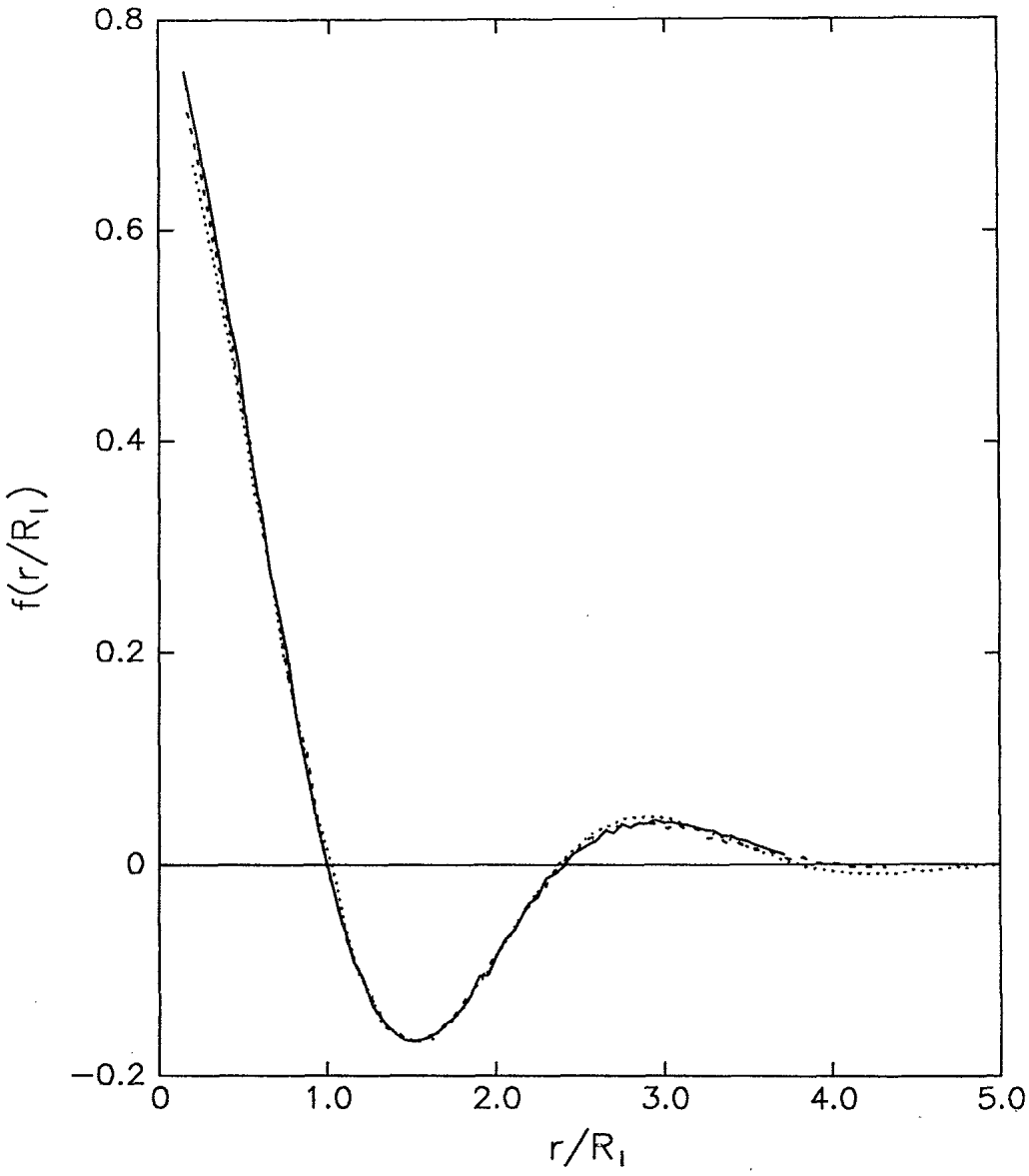

FIG. 5. The scaled correlation function for late stages in run *A*. The data is plotted for $\tau=900$ (dotted line), $\tau=1500$ (dashed line), and $\tau=2400$ (solid line).

$$\xi_{\mathbf{k}}(\tau+\Delta\tau)=\left[1-\frac{\Delta\tau}{2}\Gamma(k)-\frac{\Delta\tau}{2}\Gamma^2(k)\right]\xi_{\mathbf{k}}(\tau)+\frac{\Delta\tau}{2}\Gamma(k)\sum_{\mathbf{k}'}\sum_{\mathbf{k}''}\xi_{\mathbf{k}'}(\tau)\xi_{\mathbf{k}''}(\tau)\xi_{\mathbf{k}-\mathbf{k}'-\mathbf{k}''}(\tau)\ , \tag{3.6}$$

where

$$\Gamma(k)=\frac{2}{\Delta x^2}[\cos(k_x\Delta x)+\cos(k_y\Delta x)-2]\ .$$

$\Gamma(k)$ is the Fourier transform of the discrete Laplacian. (Note that, $\lim_{\Delta x\to 0}\Gamma(k)=-k^2$.) We are interested in stability about the homogeneous fixed point $\xi_{\mathbf{k}}=\psi_0\delta_{\mathbf{k},0}$, which corresponds to a single phase state of the system. Linearizing around this fixed point, for a critical quench ($\psi_0=0$), yields

$$\delta\xi_{\mathbf{k}}(\tau+\Delta\tau)=\sum_{\mathbf{k}'}H_{\mathbf{k},\mathbf{k}'}\delta\xi_{\mathbf{k}'}\ , \tag{3.7}$$

where

$$H_{\mathbf{k},\mathbf{k}'}=\left[1-\frac{\Delta\tau}{2}\Gamma(k)-\frac{\Delta\tau}{2}\Gamma^2(k)\right]\delta_{\mathbf{k},\mathbf{k}'}\ .$$

Fourier modes for which $|H_{\mathbf{k},\mathbf{k}}|<1$ are stable, since a small perturbation, $\delta\xi_{\mathbf{k}}$, will decay with successive iterations. Two types of instability can be identified, $H_{\mathbf{k},\mathbf{k}}>1$ and $H_{\mathbf{k},\mathbf{k}}<-1$, corresponding to tangential and subharmonic bifurcations, respectively. For the critical quench, a tangential bifurcation occurs when

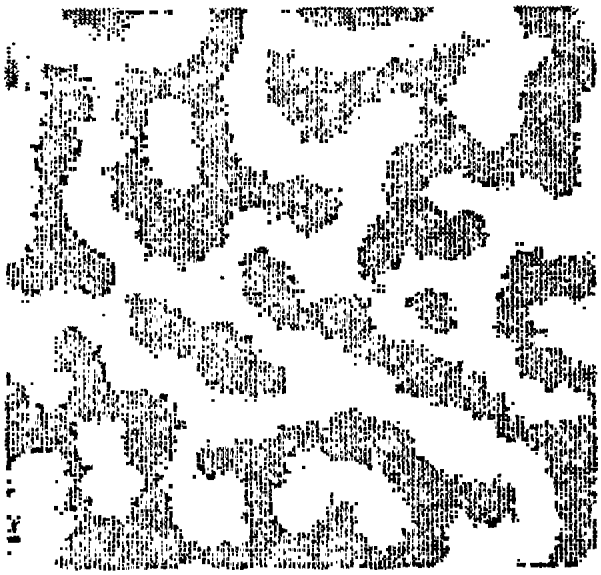

FIG. 6. Configurational snapshot for $\epsilon=0.5$ and $\tau=3000$. The shaded regions correspond to positive values of the order parameter.

$$-\Gamma(k)<1 \ . \tag{3.8}$$

The instability leads to growth of small k modes. This is consistent with Cahn's analysis[28] of the continuous equation (2.4), and reflects the onset of spinodal decomposition.

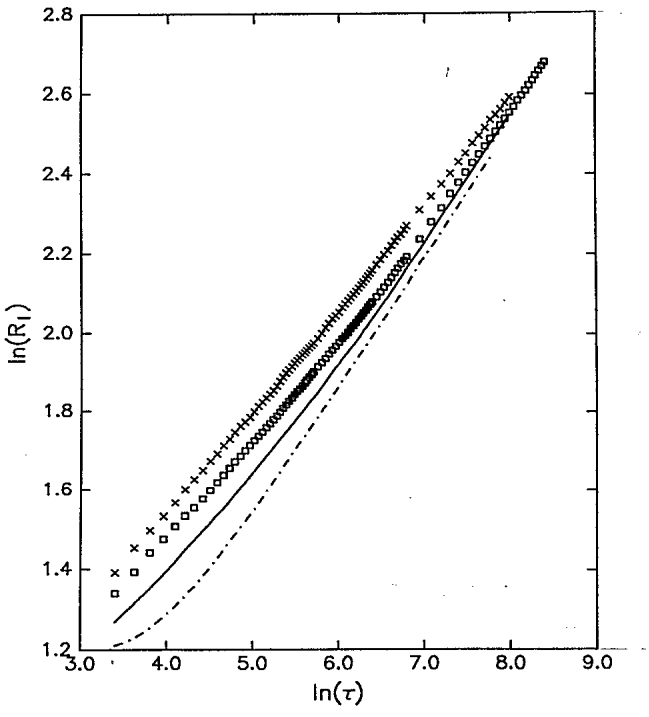

FIG. 7. The time dependence of R_1 for $\epsilon=0$ (dashed line), $\epsilon=0.05$ (solid line), $\epsilon=0.2$ (open squares), and $\epsilon=0.5$ (crosses). Increasing the magnitude of ϵ increases the time scale for the onset of linearity in the plot. The lines all appear to converge to a slope of $\frac{1}{3}$ [see Table I(a)].

More subtle is the subharmonic bifurcation condition, which has no counterpart in the continuous equation

$$-\frac{\Delta\tau}{2}\Gamma(k)-\frac{\Delta\tau}{2}\Gamma^2(k)<-2 \ . \tag{3.9}$$

Beyond the subharmonic bifurcation, the dynamics of the discrete and continuous models can be qualitatively different. In two-dimensional systems, this bifurcation can be avoided, for all k modes, by maintaining the inequality

$$\Delta\tau<\frac{(\Delta x)^4}{16-2(\Delta x)^2} \ . \tag{3.10}$$

In effect, this restricts the choice of $\Delta\tau$ for a given Δx. The constraints of (3.10) have been observed for all simulations reported here.

The mesh size is an important consideration in the simulations. Ideally, one would like to use a vanishingly small Δx. Computer limitations, however, require a more pragmatic approach. The continuous equation (2.4) inherently possesses a small length scale l, which is the width of the interface. This is clearly seen in one dimension, where the steady state solution (corresponding to a domain interface) is known: $\psi=\tanh[1/\sqrt{2}(x-x_0)]$. The interface is centered at x_0, and has a width of approximately 3 in dimensionless units.[31] This translates into an upper limit for Δx. We have investigated the dependence of the simulations on Δx in the range (0.7,2.8). For the time scales we have probed, the results converge for small Δx. However, there is a relatively sharp cutoff for $\Delta x\sim 1.4-1.7$, beyond which the simulation becomes mesh-size dependent. This trend is illustrated in Fig. 9, where we have plotted R_1 as a function of $1/\Delta x$, for $\tau=2400$. We believe that this effect is related to the inability of a large mesh size to accurately reflect the spatial gradients inherent in the interface of the continuous model. Figure 10 shows that the growth law is sensitive to the mesh size for large Δx. Most striking is the fact that the growth exponent itself is affected. It should be noted that the introduction of an underlying lattice has a physical basis in Langer's derivation[3] of model B. He defines a coarse-graining length, over which the detailed microscopic properties are averaged. At this level, the mesh size used in our simulations can be interpreted as a coarse-graining length.

The subharmonic bifurcation condition imposes a restriction on the time step, $\Delta\tau$, which is strongly dependent on the mesh size. For small ϵ, this appears to be the only constraint on the time step. In Fig. 11 the results of simulations for $\Delta\tau=0.3$ and $\Delta\tau=0.03$ are compared ($\epsilon=0.05$). The data are identical, within the accuracy of the statistics. For large ϵ, the linear perturbation analysis is insufficient. The noise introduced at each time step has an average magnitude of $(\epsilon\Delta\tau)^{1/2}/\Delta x^2$. This finite amplitude perturbation can lead to divergences in the simulation if $\Delta\tau$ is too large.

IV. DISCUSSION

These simulations shed considerable light on the problem of domain growth. Runs A through D show that the

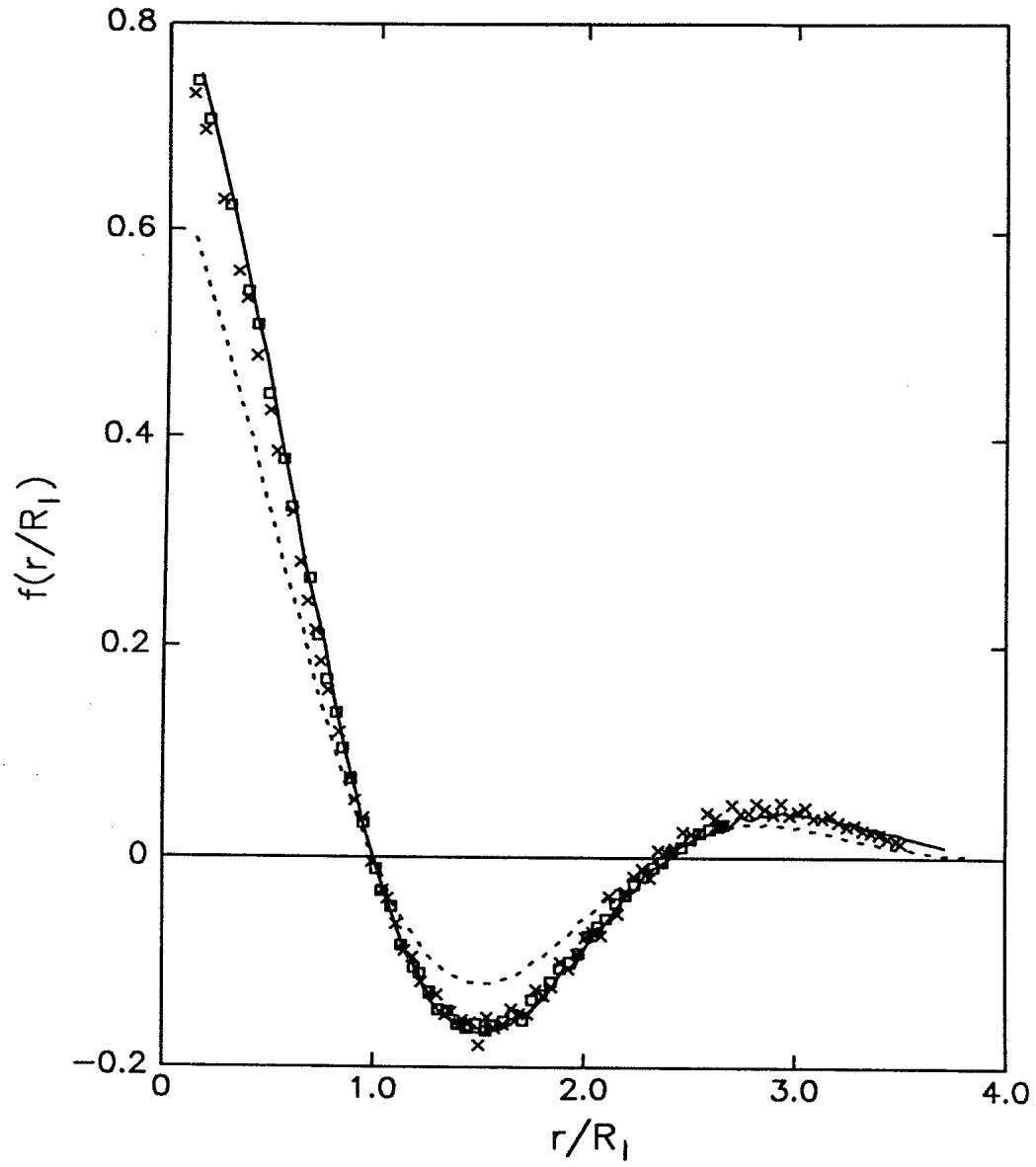

FIG. 8. Late-stage scaling function for $\epsilon=0$ (solid line), $\epsilon=0.05$ (open squares), and $\epsilon=0.2$ (crosses). The dashed line corresponds to the latest time probed for $\epsilon=0.5$ (this simulation has not reached the scaling regime).

late-stage growth exponent is $\frac{1}{3}$ for model B. This is consistent with computer simulations[11,14,15,17] and experiments[20–24] on other systems with a scalar conserved order parameter. There is strong evidence that it is, in fact, a universal feature of such systems.

An effective exponent can be introduced to describe the intermediate stages of domain growth. Figures 3 and 7 show that the exponent varies continuously with time. However, this description may be somewhat misleading since scaling is not established until the very late stages. In particular, for the range of ϵ we have studied, the pair-correlation function does not scale during the time scales where $n_{\text{eff}}<\frac{1}{3}$. This result has important theoretical implications, since it discounts the possibility of an (intermediate) scaling regime where the growth exponent is $\frac{1}{4}$.

It has been argued[5,11] that the approach to asymptotic growth of the average domain size is given by a power series expansion in $t^{-1/3}$:

$$R(t)=A_1t^{1/3}+A_2+A_3t^{-1/3}+\cdots . \tag{4.1}$$

This prediction has been verified in spin-exchange Ising simulations[11,14] and in experiments on a binary alloy.[24] Figure 12 shows a plot of R_1 as a function of $\tau^{1/3}$ for our data. For $\epsilon=0$, the data are remarkably linear over the late-stage regime. During these time scales, the first two terms in the expansion correctly describe the growth. As ϵ is increased, the onset of linearity is pushed further in time, indicating the increasing importance of higher-order terms. The final slope attained by the data for each ϵ is given in Table II. The similarity of the slopes is a

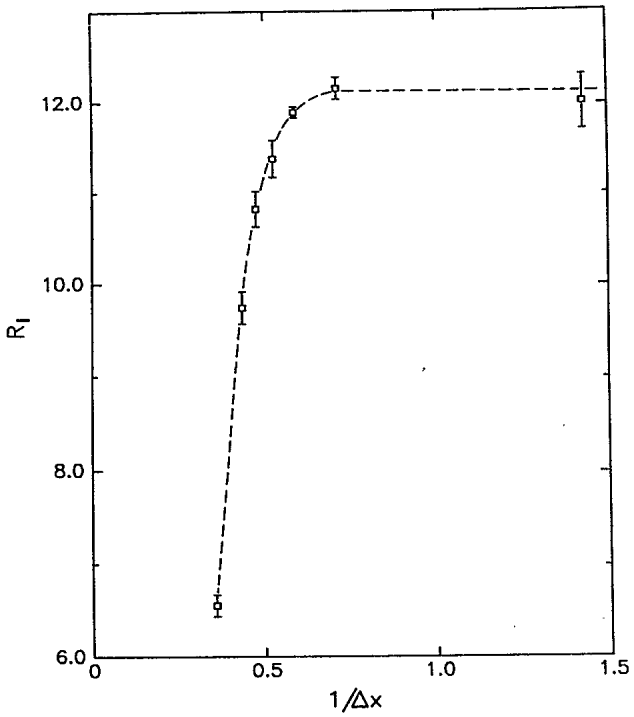

FIG. 9. Comparison of R_1 for different values of Δx at $\tau=2400$. The appropriate simulation parameters are given in Table I(b). The plot shows convergence for small Δx. (The dashed line is intended as a guide for the eye.)

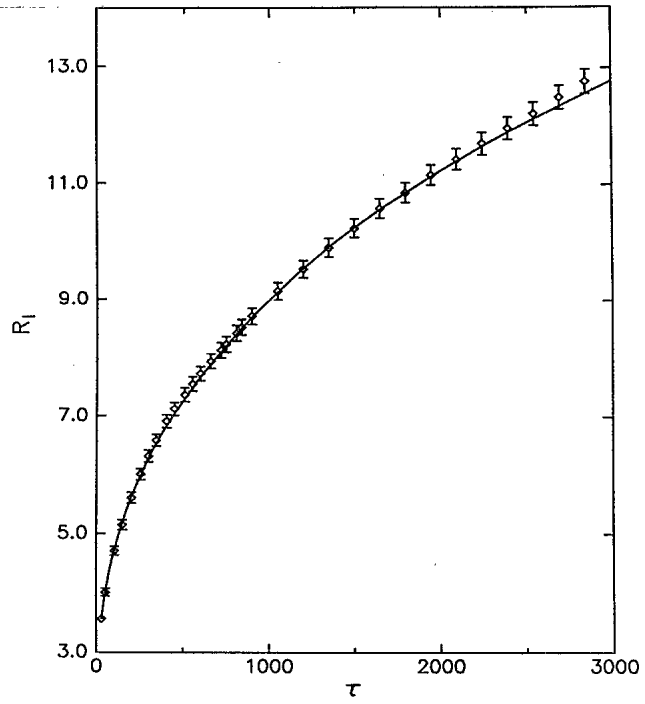

FIG. 11. Comparison of the time dependence of R_1 for run B (solid line) and run K (open diamonds). The plot shows that changing $\Delta\tau$ does not affect the results of the simulation (see text).

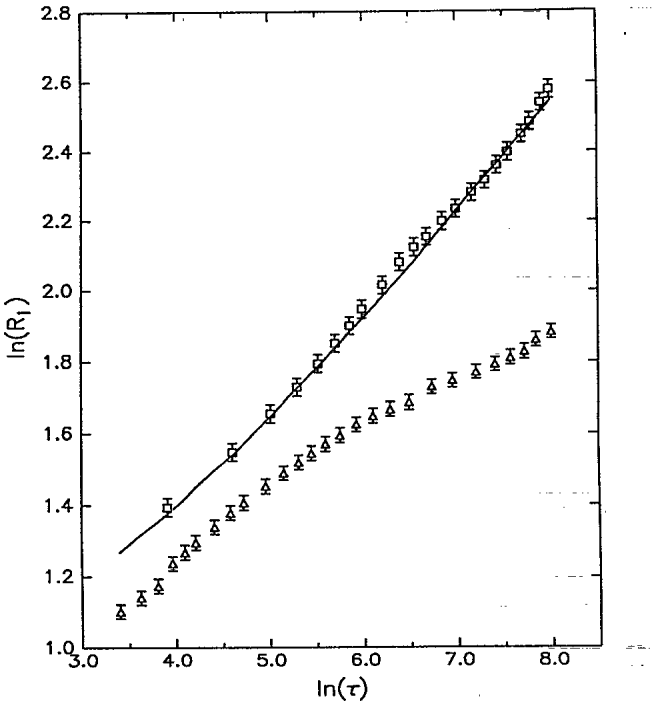

FIG. 10. Time dependence of R_1 for $\Delta x=0.7$ (open squares), $\Delta x=1.7$ (solid line), and $\Delta x=2.8$ (open triangles). The data are taken from runs E, B, and J, respectively. For large Δx there is a change in the growth law.

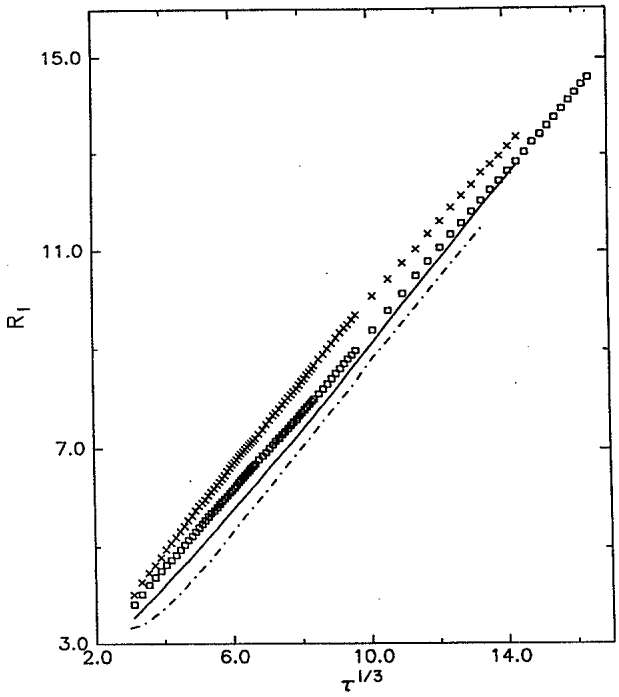

FIG. 12. R_1 as a function of (time)$^{1/3}$ for $\epsilon=0$ (dashed line), $\epsilon=0.05$ (solid line), $\epsilon=0.2$ (open squares), and $\epsilon=0.5$ (crosses). The slopes at late times are given in Table II.

TABLE II. Growth coefficient A_1 [see Eq. (4.1)] for various values of ϵ.

Run	ϵ	A_1
A	0	0.84±0.02
B	0.05	0.85±0.02
C	0.2	0.81±0.03
D	0.5	0.81±0.05

strong indication that the leading order coefficient, A_1, is independent of ϵ. When this information is combined with the analysis of the scaling functions, we are led to the conclusion that fluctuations are irrelevant to asymptotic domain growth.

The strength of thermal noise does play an important role in the early and intermediate stages of phase separation. With increasing ϵ, domain growth is enhanced and the time scale for the onset of scaling is increased. Large ϵ corresponds to a quench near the critical point of the model. Thus it can be expected that the transition regime will become increasingly more important as the critical point is approached.

The breakdown of scaling at intermediate times may be related to the establishment of sharp walls. The interfacial width, l, introduces a second length scale into the problem, which leads to a more general scaling ansatz,

$$g(r,t)=f(r/R,l/R)\ . \tag{4.2}$$

Since the time dependence of l is different from that of R, it is only when $l/R\rightarrow 0$ that Eq. (3.3) is valid. This limit is always obtained for sufficiently large times (since l decreases to a constant with time). The ratio of the two length scales becomes a natural small expansion parameter for a late-stage theory of the pair correlation function. It can be shown analytically that model B predicts $R\sim t^{1/3}$ in the limit $l/R\rightarrow 0$. As ϵ is increased, the walls become broader due to the noise. This increase in l affects corrections to asymptotic growth and may be related to the increase in the time scales for the onset of scaling as seen in the simulations.

The simple finite-difference algorithm produces efficient (vector) code. However, there are some limitations, such as the subharmonic bifurcation and the mesh-size effect. As with any simulation, one must be careful to avoid spurious solutions. It should be pointed out that model B contains only one dimensionless parameter, which is related to the strength of fluctuations. Consequently, a faithful computer simulation of the model should admit only one parameter through which the physics can change (i.e., ϵ). Variation of other parameters (for example, Δx and $\Delta\tau$) should yield consistent results when appropriately interpreted. Conversely, if one assumes the discrete lattice is fundamental (as in the work of Langer[3]), then our data suggest that the coarse-graining length is not important in the dynamics as long as it is much less than the interfacial width.

V. CONCLUSIONS

The process of phase separation in model B is an intriguing theoretical problem, which eludes complete understanding. The method of finite differences provides an effective algorithm for studying the problem numerically. Using this technique, we have attempted to gain some insight into domain growth and scaling in the model.

We find that during late stages, the domains coarsen as a power of time. The measured (asymptotic) exponent of $\frac{1}{3}$ places the model in the same universality class as the spin-exchange kinetic Ising model and many other systems with a scalar conserved order parameter. We also find that scaling of the pair-correlation function is an asymptotic result. The scaling function and the asymptotic growth law are independent of the strength of the thermal noise. We believe that the interfacial width plays an important role for intermediate times and leads to time-dependent corrections to dynamic scaling. It would be of considerable interest to make a detailed comparison with experimental systems and computer models that are expected to map onto model B.

Note added in proof. It has recently come to our attention that E. T. Gawlinski, J. D. Gunton, and J. Viñals have carried out a similar numerical study of this model for $\epsilon=0.1$. They have also concluded that the asymptotic growth exponent is $\frac{1}{3}$ (private communication).

ACKNOWLEDGMENTS

We would like to thank Gian-Luca Oppo, Raymond Kapral, and Martin Grant for useful discussions. We gratefully acknowledge IBM-Canada for use of an IBM-3081. This work is also supported by the Natural Sciences and Engineering Research Council of Canada.

[1]J. D. Gunton, M. San Miguel, and P. Sahni, in *Phase Transitions and Critical Phenomena,* edited by C. Domb and J. L. Lebowitz (Academic, London, 1983), Vol. 8, p. 267 and references therein.

[2]I. M. Lifshitz and V. V. Slyosov, J. Phys. Chem. Solids **19**, 35 (1961).

[3]J. S. Langer, Ann. Phys. **65**, 53 (1971).

[4]E. D. Siggia, Phys. Rev. A **20**, 595 (1979).

[5]J. A. Marqusee and J. Ross, J. Chem. Phys. **79**, 373 (1983); **80**, 536 (1984); J. A. Marqusee, *ibid.* **81**, 976 (1984).

[6]For a recent review, see P. W. Voorhees, J. Stat. Phys. **38**, 231 (1985).

[7]K. Binder and D. Stauffer, Phys. Rev. Lett. **33**, 1006 (1974).

[8]J. S. Langer, M. Bar-on, and H. D. Miller, Phys. Rev. A **11**, 1417 (1975).

[9]K. Binder, Phys. Rev. B **15**, 4425 (1977); Rep. Prog. Phys. **50**,

783 (1987).
[10]H. Furukawa, Prog. Theor. Phys. **59**, 1072 (1978); Adv. Phys. **34**, 703 (1985).
[11]D. A. Huse, Phys Rev. B **34**, 7845 (1986).
[12]G. F. Mazenko, O. T. Valls, and F. C. Zhang, Phys. Rev. B **31**, 4453 (1985); **32**, 5807 (1985).
[13]J. L. Lebowitz, J. Marro, and M. H. Kalos, Acta Metall. **30**, 297 (1982).
[14]J. G. Amar, F. E. Sullivan, and R. D. Mountain, Phys. Rev. B **37**, 196 (1988).
[15]S. W. Koch, R. C. Desai, and F. F. Abraham, Phys. Rev. A **27**, 2152 (1983).
[16]M. Schoebinger, S. W. Koch, and F. F. Abraham, J. Stat. Phys. **42**, 1071 (1986).
[17]Y. Oono and S. Puri, Phys. Rev. Lett. **58**, 836 (1987). (The definition of domain-wall thickness used here is mesh-size dependent.)
[18]A. Milchev, D. W. Heermann, and K. Binder (unpublished).
[19]G. F. Mazenko and O. T. Valls, Phys. Rev. Lett. **59**, 680 (1987).
[20]Y. C. Chou and W. I. Goldburg, Phys. Rev. A **23**, 858 (1981).
[21]N. C. Wong and C. M. Knobler, Phys. Rev. A **24**, 3205 (1981).
[22]A. Craievich and J. M. Sanchez, Phys. Rev. Lett. **47**, 1308 (1981).
[23]S. Katano and M. Iizumi, Phys. Rev. Lett. **52**, 835 (1984).
[24]B. D. Gaulin, S. Spooner, and Y. Mori, Phys. Rev. Lett. **59**, 668 (1987).
[25]R. Kapral, Phys. Rev. A **31**, 3868 (1985); G.-L. Oppo and R. Kapral, *ibid.* **33**, 4219 (1986); R. Kapral and G.-L. Oppo, Physica D **23**, 455 (1986); G.-L. Oppo and R. Kapral, Phys. Rev. A **36**, 5820 (1987).
[26]O. T. Valls and G. F. Mazenko, Phys. Rev. B **34**, 7941 (1986).
[27]P. Meakin, H. Metiu, R. G. Petschek, and D. J. Scalapino, J. Chem. Phys. **79**, 1948 (1983); R. G. Petschek and H. Metiu, *ibid.* **79**, 3443 (1983).
[28]J. W. Cahn and J. E. Hilliard, J. Chem. Phys. **28**, 258 (1958); H. E. Cook, Acta Metall. **18**, 297 (1970); see also, Ref. 1.
[29]M. Grant, M. San Miguel, J. Viñals, and J. D. Gunton, Phys. Rev. B **31**, 3027 (1985).
[30]For a given run, the error in the radius, σ_R, is approximated by $\sigma_R = \sigma_{\text{trial}}/\sqrt{N_{\text{trial}}}$, where N_{trial} is the number of trials in the run.
[31]We define the domain wall as the region over which the order parameter varies from $A\psi_+$ to $A\psi_-$, where $\psi_\pm$ are the final equilibrium values of the order parameter and A is (arbitrarily) set at 0.75.
[32]O. G. Mouritsen, Phys. Rev. Lett. **56**, 850 (1986).
[33]R. H. Morf and E. P. Stoll, in *Numerical Analysis,* Proceedings of the Colloquium on Numerical Analysis, Lausanne, edited by J. Descloux and J. Morti (Birkhauser Verlag, Basel, 1977), p. 139; see also, Ref. 26.